



Enzymatic tandem systems engineered from mesoporous thin films: Synergy leading to efficient starch-electricity conversion



Martín G. Bellino^{a,b,*}, Sofia Municoy^b, Galo J.A.A. Soler-Illia^a

^a Gerencia Química—Centro Atómico Constituyentes, Comisión Nacional de Energía Atómica, Av. Gral Paz 1499, San Martín, B1650KNA Buenos Aires, Argentina

^b Departamento de Micro y Nanotecnología, Comisión Nacional de Energía Atómica, Av. Gral Paz 1499, San Martín, B1650KNA Buenos Aires, Argentina

ARTICLE INFO

Article history:

Received 3 February 2016

Received in revised form 1 April 2016

Accepted 6 April 2016

Available online 8 April 2016

Keywords:

Mesoporous materials

Enzymatic tandem

Biofuel cells

Nanocomposites

Thin films

ABSTRACT

The synergetic combination of nanomaterials with biomolecules, which is inherent to natural systems is a challenging and thriving field. In Nature, a wide variety of enzymes work together in multi-step reactions into sophisticated subcellular compartments. Mesoporous Oxide Thin Films (MOTF) permit to divide the space in highly ordered functional domains, providing a promising multiscale scaffold to host enzymes. However, the emergent properties of MOTF in which enzymes are hierarchically ordered and coupled together have not been explored yet. Here, we demonstrate how the confined cavities of an organized multilayer of MOTF, in resemblance to living cell compartments, can be used to host two different enzymes to activate a cascade of enzyme reactions that do not proceed under free enzyme conditions. Transformation of complex carbohydrates such as starch to electricity is widely recognized to be an important technological objective. The MOTF multilayer was used as a bionanofactory, achieving a starch-fuelled biofuel cell that yields the best performance obtained so far, jointly with reduced operating fuel requirement. This development demonstrates that enzymatic pathways can be engineered from mesoporous thin film architectures, opening the way for evolving bio-active surfaces in packaging, sensors, prosthetics, or bioMEMS among other exciting applications.

© 2016 Elsevier Ltd. All rights reserved.

1. Introduction

Mesoporous Oxide Thin Films are open both to large-area integration with matter and the miniaturization of materials and devices [1,2]. The confined spaces of MOTF can be used to precisely include functional nano-objects, such as enzymes [3–5] or nanoparticles [6–8]. In living cells multi-enzymatic systems spatially localized within subcellular organelles catalyze crucial processes that involve multiple reaction steps [9,10]. Mimicking this multi-enzyme architectures, a number of examples have been reported co-entrapping multiple enzymes within liposomes [11] or solid particles [12–14] allowing improved efficacy. However, most examples rely in soft-matter derived nanosystems in suspension, which have limitations regarding control over dispersion, or recovery. On the other hand, robust scaffolds able to host a multi-enzymatic system are desirable, in order to make an enzyme cascade work together, with high stability and recoverability. The

concept of tandem enzymatic reactions has been demonstrated, and even applied to fuel cells [15]. However, a robust mesopore system in which different enzymes can be lodged independently and act sequentially is significant for the further development of versatile bioactive coatings. Interestingly, a thin film mesoporous ceramic scaffold is mechanically sound and can be easily integrated with the usual processing methods in electronics or micro- and nanofluidic biodevices. The matrix immobilization of a controlled positional assembly of enzyme machineries permits that intermediates generated by one enzyme can be promptly transformed by the following one, preventing the diffusion of intermediates to the surroundings. This synergic behaviour, which is essential in living cells [9], would be an innovative approach for the creation of novel biofunctional films in a wide range of advanced applications with inedited performance. A first demonstration of synergism between mesoporous thin films and enzyme systems reported here is performed developing a hybrid multi-enzymatic nanostructure that “metabolizes” a complex carbohydrate to extract electricity with unprecedented efficiency.

An enzymatic fuel cell (EFC) is the offspring of biotechnology and fuel cell development towards versatile power supplies. Conventional enzyme composite anodes give good performance with simple carbohydrates as glucose as fuel [15–18]. Generally,

* Corresponding author at: Gerencia Química—Centro Atómico Constituyentes, Comisión Nacional de Energía Atómica, Av. Gral Paz 1499, San Martín, B1650KNA Buenos Aires, Argentina.

E-mail address: mbellino@cnea.gov.ar (M.G. Bellino).

glucose fuel is oxidized by glucose oxidase (GOx) and the electrons are transferred to the electrode utilizing redox-active compounds as mediators. Nature provides numerous potential power sources in the form of complex carbohydrates and the challenge is their efficient conversion into electrical energy. Starch plays essential roles during the life cycle, as the main storage carbohydrate in plants [19]. In order to use the energy contained in these complex carbohydrates, living organisms must metabolize, or break down, the structure of these large macromolecules. Starch is converted into glucose and utilized by all the cells of the organism to extract energy. There are, however, very few examples of starch fuelled BFCs [20–22]. The development of high power starch BFCs with versatile system design (e.g. membrane-less and mediator-less operation without the need of adding mediator, thin film architecture and low cost) is highly desirable.

As proof of concept, this Communication synergistically combines a two layer mesoporous thin film with a bi-enzyme system (glucoamylase and glucose oxidase) for coupling process of starch degradation and electrical conversion steps that do not proceed with free enzymes in similar conventional conditions. Consequently, the high power of the resulting starch biofuel cells exceeds by far to those previously reported, together with capability to operate at extremely low fuel concentrations.

This example of a mesoporous films to make enzymatic pathways work more effectively has strong immediate implications for the rational design of novel bioactive nano-coatings to advanced applications.

2. Results and discussion

A two-layer porous nanoreactor was prepared by placing a glucose electrode based on a hierarchically mesoporous titania thin film in a bottom layer. The hierarchical film presents large pores

that host Glucose Oxidase (GOx) and smaller mesopores embedding silver nanoparticles, as recently reported [23]. On top of the titania layer, an amylase functionalized mesoporous silica thin film was placed. The porous TiO₂/SiO₂ bilayers (substrate-titania-silica) were deposited by dip-coating from alcohol-water acidic solutions containing the inorganic precursor and polymeric non-ionic templates. Films were produced and processed under controlled environmental conditions and thermal treatment, following well-established protocols (see details in the Experimental Section) [24,25]. The average pore diameters measured by TEM and ellipsometric porosimetry analysis (EPA) was 11 nm for the silica top layer, and a hierarchical pore size distribution with diameters of 13 and 38 nm for the bottom titania layer. The top layer was 130 nm thick, 51% porous and the bottom layer was 78 nm thick, 47% porous according to ellipsometry and EPA (see Figs. 1a and S1 in Supplementary content). The subsequent steps involved depositing Ag nanoparticles through a TiO₂-photocatalysis reaction procedure previously reported [6,7], which are selectively located, occupying the small size mesopores into the titania bottom layer [6,24], showing the typical surface plasmon resonance of silver nanoparticles (see Supplementary content Fig. S2). Finally, layers were loaded with GOx and amylases by subsequent adsorption from each aqueous enzyme solution.

The relatively large GOx macromolecule (5.1 nm Stokes radius) [26] is excluded from the small pore silica located in the top layer due to the interpore necks which are smaller than the hydrodynamic enzyme diameter, but the large pores interconnected through much wider necks of the titania bottom layer admit the large-size enzyme incorporation into this hierarchical titania film (see Supplementary content Fig. S3) [3,23]. The larger mesopores evenly distributed along the whole lower film thickness and interconnected by large interpore neck sizes [25], also permit the lateral diffusion of nano-species into the lower layer [27]. The top layer of

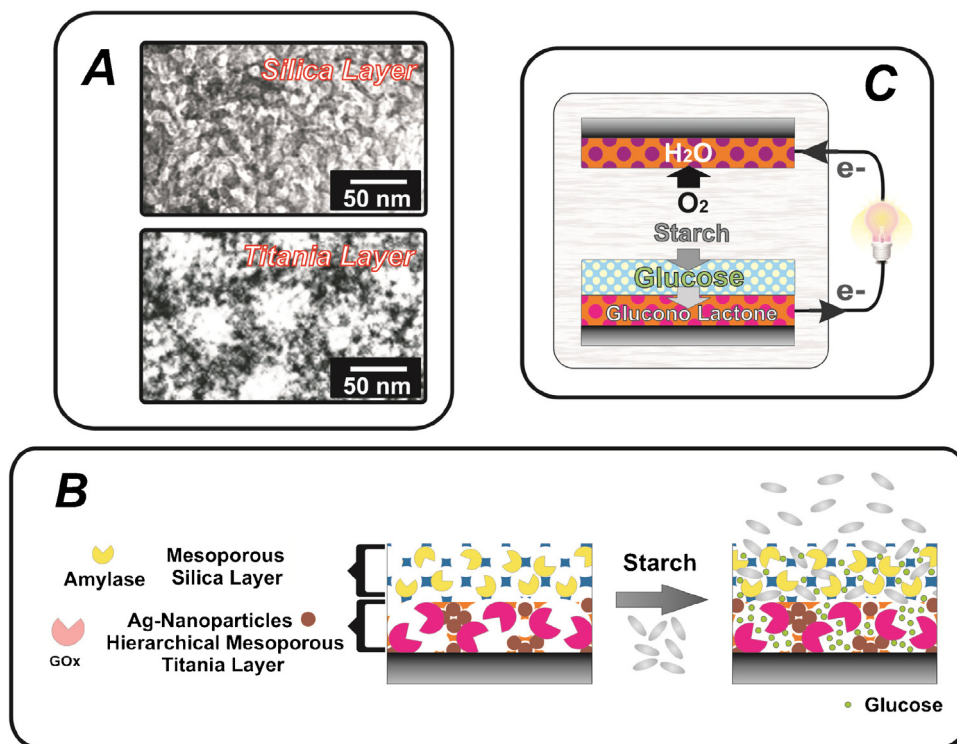


Fig. 1. (A) Transmission electron images illustrating the different mesoporous architecture in each layer scaffold used in this study. (B) Schematic illustration of nanoreactor used to process starch to direct conversion into electricity and (C) single compartment starch EFC. The system allows to an *in situ* biocatalytic cascade in the anode nanostructure which hydrolyzes starch to glucose into the top (amylase-functionalized silica) layer that is then oxidized in the lower (GOx-functionalized Ag/titania) layer and the electrons are transferred from the GOx to the electrode. At the cathode, electrons are transferred from electrode to laccase where dioxygen is reduced to water.

the nanostructure excludes the GOx but can act as a host layer for smaller proteins such as amylases [4], (see Supplementary content Fig. S3), which typically hold a Stokes radius of *ca.* 3.3 nm [28].

The activities of the biofunctionalized nanostructure to starch degradation were monitored by the well-known starch-iodine colorimetric method [4,29]. Biofunctionalized nanostructures immersed in starch solutions showed a significant capability to degrade starch. At pH 7 and room temperature (20 °C), bilayered films degrades per cm² nearly the same amount of starch that 6 μg of free amylase (see Supplementary content Fig. S4), in good agreement with the enzyme loading (6.4 μg/cm²), indirectly derived by spectroscopic measurements of protein supernatant solution after adsorption (see Supplementary content Fig. S3). On the contrary, the activity of biofunctionalized nanocomposite films without the mesoporous silica layer was negligible, according to the inability to incorporate significantly the amylases after GOx immobilization and highlights the importance of the mesoporous silica layer in these nanostructures.

To demonstrate that the double layer bienzymatic nanostructure presents an intrinsic capacity to direct transformation of starch to electricity (sketched in Fig. 1b), we carried out electrochemical measurements. Consecutive reactions of starch and glucose were performed by glucoamylase (GA) and GOx, respectively. When starch was added, it was hydrolyzed by GA, producing glucose, which was further oxidized via GOx where the electrons are transferred to electrode.

The importance of mesoporous scaffold in promoting the tandem enzymatic process is vividly illustrated in Fig. 2a. These biofunctional nanostructures, potentiostated at -0.1 V, exhibited a strong anodic current response to starch additions (1%) indicating their ability to achieve a multi-step enzymatic process that turn complex carbohydrates to charge transference to the electrode. The biofunctional nanostructure showed a fast and sensitive response to starch, reaching up to 90% of the maximum steady-state current in 180 s. In contrast, hardly any activity was detected when supported amylases were replaced with the equivalent activity of free enzymes (Fig. 2a). Therefore, a key element of the strategy here presented is the closed spatial proximity of the complementary enzymes that is achieved in this multilayer mesoporous scaffold. Similar experiments performed by replacing GOx and both enzymes for equivalent activity of enzymes in solution showed no activity, reinforcing the hypothesis that all components of the system (matrix scaffold and bi-enzyme pathway) are necessary to produce an efficient biochemical catalysis. These result shows that this nanostructured film constitutes an efficient scaffold to enzymatic tandem leading to a speeded-up fuel process that does not occur (at similar experimental conditions) in a soluble system. This interesting behaviour can be attributed to an increase in the catalytic efficiency by proximity effect where a short distance decreases the diffusion time to the nearest complementary enzyme [9]. This result obtained in the nanoengineered bilayer shows a promising direction to further development of novel bioactive coating and biodevices.

The stability of the bionanostructure, and hence the reproducibility of electrical system was evaluated by periodically measuring current density. The electrodes were stored in buffer solution at room temperature for a given time, and new current measurements were performed. After a slight initial decrease during the first day, current density maintained more than 90% of its initial value after storage for 10 days (Fig. 2b). This illustrates the good stability of the bioelectrode system.

In order to take advantage of the latent properties described above for direct conversion of starch into useful electric power, we used the bi-enzymatic electrode described above as an anode associated with a laccase composite cathode where dioxygen is reduced to water, in an arrangement similar to our recently reported work

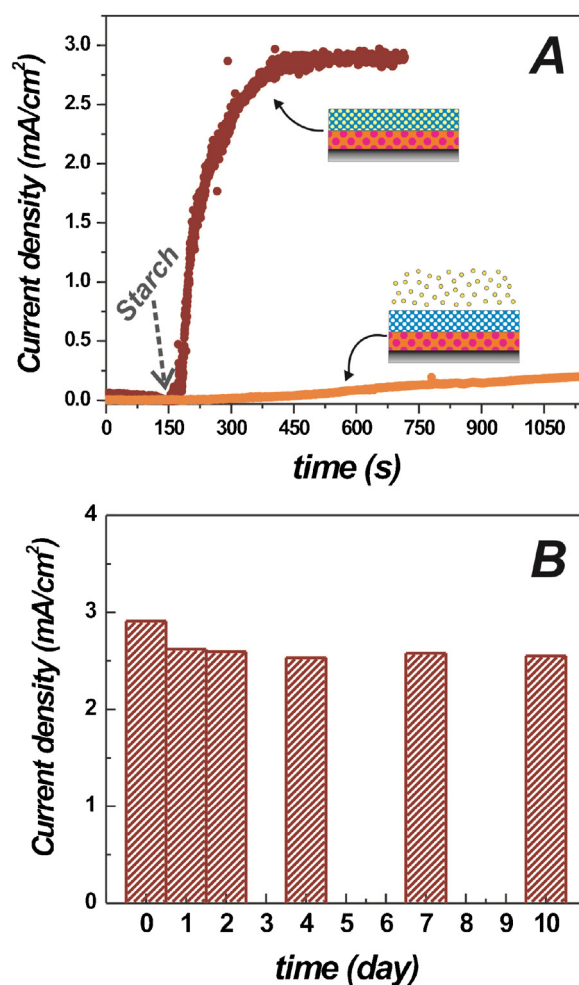


Fig. 2. Bioelectrode performances. (A) Chronoamperometric response for a bioelectrode after addition of 1% weight starch solution, at -0.1 V versus SCE by enzymes associated with the mesoporous scaffold and their corresponding free amylase condition. (B) Evolution of current density of bioelectrode at 0V versus time. The performances of the bioelectrodes were examined in phosphate buffer (0.2 M, pH 7, 20 °C).

[23]. The biocathode and bioanode were immersed in a one-compartment cell containing phosphate buffer solutions (pH 7) containing starch at 20 °C (Fig. 1c), allowing to a membrane-less and mediator-less starch/O₂ biofuel cell. As expected, without amylase functionalization these biofuel cells showed no activity in presence of starch. The effect of the catalyst layer is presented in Fig. 3a. Typical cell performance exhibited open circuit voltages of 0.92 V which is correspondent with the difference between the potentials of the two redox biocatalysts [30]. The variation of the power density as a function of current density presents the usual shaped curve relative to a fuel cell with a maximum of 380 μW cm⁻² at 0.62 V when in contact with 1% weight starch solutions. The present power results compare favourably with any reported methods for using starch fuels in EFCs (see Supplementary content Fig. S5). Compared to similar configurations based on carbon nanotube scaffolds [20], the performances here presented represent an increase of two orders of magnitude in terms of power density. In addition, such power densities here reported are one order of magnitude higher than those obtained in compartmented (by using ion selective membranes) and mediated starch EFCs [21], and fourfold higher than the power density recently obtained for EFCs utilizing multi-enzymatic mediator-carbonaceous composite thick electrodes [22].

Please note that a solution of 1% starch will turn into *ca.* 50 mM glucose upon completing the hydrolysis, corresponding to

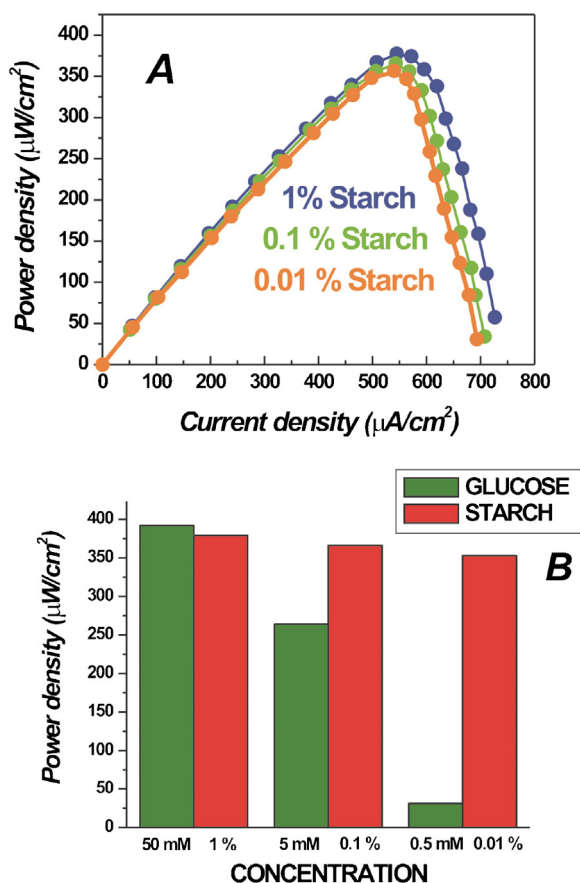


Fig. 3. Biofuel cell performances. (A) Dependence of power density on current density for a biofuel cell in a quiescent pH = 7 phosphate buffered starch solutions under air at 20 °C after 5 min of starch addition. (B) Compared power densities of biofuel cells in the presence of different concentrations of starch with the glucose concentrations corresponding to completed starch saccharification.

a substrate saturating glucose oxidase conditions. Remarkably, the performance under starch 1% of EFC here developed is comparable to obtained for the same cells operated on 50 mM glucose (see glucose-fuelled EFC performance in Supporting content Fig. S6), emphasizing that the nanostructured scaffold here utilized is highly efficient to favour enzymatic cascade pathways. Fig. 2a shows the performance of the EFC in phosphate buffer containing starch concentrations (0.1–0.01 wt%) that correspond to a final concentration of glucose after saccharification of ca. 5–0.5 mM, a concentration range markedly lower than the one corresponding to the saturating glucose condition. Interestingly, even at low starch concentration the EFC practically maintains the power output attained on saturated substrate conditions (see Fig. 3a), while the cell presents significantly weaker power values when exposed to the equivalent amounts of glucose (see Supplementary content Fig. S6). Fig. 3b compares the power density of EFCs operating on starch as the fuel with those in which the fuel was replaced by glucose concentrations corresponding to completed starch saccharification. Compared with corresponding glucose fuelled EFCs, starch EFCs demonstrated higher power densities up to a factor 11 for 0.01% starch concentration. We attribute these results to the pore architecture that limits the diffusion of the *in situ* generated glucose, keeping an elevated glucose concentration within the film, and acting thus as a concentrator for the subsequent oxidation reaction that takes place in the layer beneath. This demonstrates that the confined nanopores and crowded environments typical of a mesoporous system provide a unique and tuneable nanoarchitecture that presents an extraordinary fuel efficiency. Confinement

and precise functional positioning at the nanoscale are key features in living cell metabolic efficacy [31].

In order to test the stability of the EFC, the power density dependence on current density was recorded after 10 days storage of EFC in the buffer solution at room temperature. Fig. 4a shows only a 7% decrease for the maximum power density, reaching 355 $\mu\text{W}/\text{cm}^2$ at 0.58 V. In addition, we studied the evolution of the EFC voltage under a constant current discharge of 500 $\mu\text{W}/\text{cm}^2$ near where the maximum power density was achieved. The cell was tested along 30 h in continuous operation, after which we observed only an 8% loss in voltage output (see Fig. 4b). Most of the decay is attained in the first two hours, then voltage levels off, showing stabilization of the biofuel cells maintaining the current discharge. Although the voltage decreased slowly to 0.63 V after three hours, these biofuel cells were able to maintain the current discharge at low fuel concentration (see Fig. 4b), emphasizing that fuel harnessing capability is remarkably efficient. Despite the fact that enzyme functionalization may actually hinder dissolution of the inorganic matrix, it can be argued that the instability of mesoporous thin films in aqueous media represents a liability of these biocatalysts for long-term applications. Nonetheless, our data clearly show that this starch EFC exhibits long-term stability for a biofuel cell, maintaining a significant power output during several days storage and over several hours operating time.

The performance of the tandem biofuel cells at different temperature and pH values are shown in Fig. 4c and d. The maximum power density was achieved at ca. 37 °C and pH 7. Remarkably, these BFC retain high power densities at extreme temperature and pH values as a consequence of the stabilizing effect of immobilization [4,5]. The ability to retain bioactivity in broad ranges provides advantages to integrate these biocatalytic films for advanced applications.

3. Summary

In summary, we introduced MOTF as a robust yet versatile scaffold to produce tandem enzymatic systems that permit a cascade enzymatic process. The cascade reaction that could not be catalysed in a free enzyme condition was found to be effectively activated when the enzymes were assembled on the MOTF scaffold. These experiments provide an excellent example of the possibilities opened by MOTF-based architectures to achieve multi-enzymatic nanosystems. The self-sustaining nanofactory-system is designed by selectively locating enzymes and active nanoparticles in mesoporous layers, using pore size, surface charge and selective reactivity as synthetic tools. This permits to build a tandem system with well-defined functional domains. A first catalytic reaction takes place in the top layer, where the starch fuel is abundant. The intermediate reaction products and the electron transfer process take place separately in the bottom layer. The present *in situ* fuel processing in this nano-engineered anode shows the feasibility of versatile EFCs fuelled by natural polymers such as starch, with substantial advantages including high performance and simple system design, together with higher fuel harnessing capability and it is a promising step toward practical biofuel cells capable to operate at extremely low fuel concentrations.

It is worth mentioning that the assembly system is modular and scalable, and can therefore be extended to numerous enzyme tandem pathways giving rise to a novel generation of biofunctional coatings and devices in many exciting areas of current research, which ranges from a variety of applications in biosensors, synthetic biology and responsive materials to industrial biocatalysis, prosthetics and intelligent packaging. In addition, the production and processing steps used are compatible with those used in electronics and microfluidics, permitting to incorporate these BFC in devices. Finally, we report, indeed, a first step in the integration of

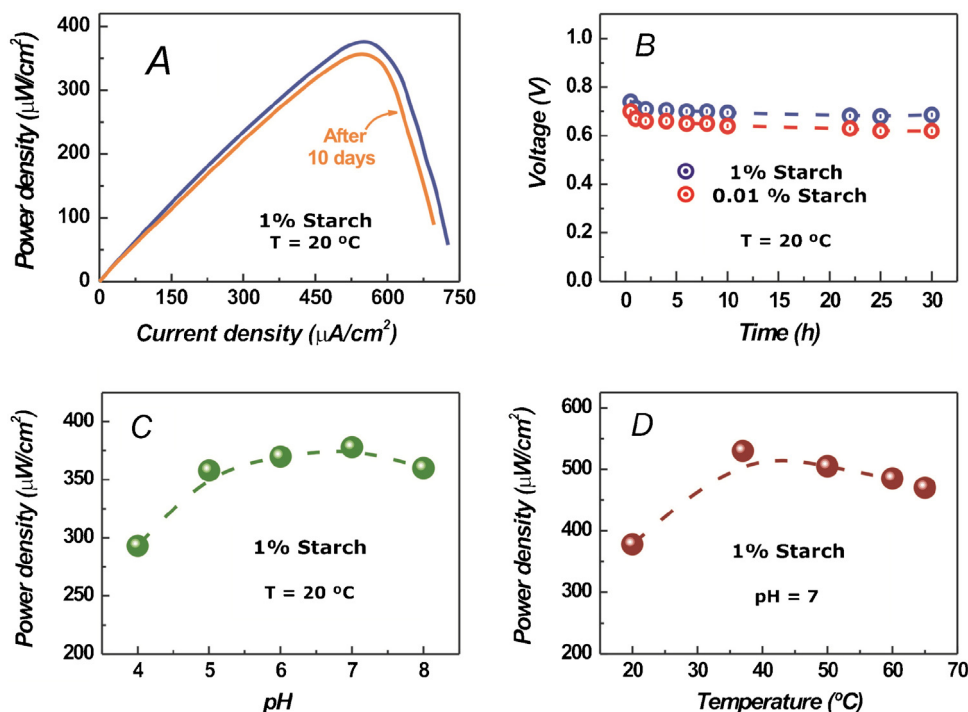


Fig. 4. Biofuel cell stability. (A) Dependence of power density on current density in 1% starch solution pH = 7 phosphate buffered under air at 20 °C, before (blue) and after 10 days (orange). (B) Long-term performance of voltage on time for continuous discharge under $500 \mu\text{A cm}^{-2}$ in starch solutions pH = 7 phosphate buffered under air at 20 °C. Influence of (C) pH and (D) temperature on the power density of biofuel cells in 1% starch solutions. (For interpretation of the references to colour in this figure legend, the reader is referred to the web version of this article.)

different aspects of cellular biochemistry such as enzymatic cascades, confinement and crowding on MOTF that could in the short term lead the emergence of unique multi-compartment nanosystems that mimic complex living cell behaviour.

4. Materials and methods

Synthesis of mesoporous layers. Prior to deposition, soda-lime glass slides (76 mm long, 26 mm wide, 1.1 mm thick) were thoroughly washed with Dextran followed by successive rinsing in water, ethanol, and acetone. Hierarchical mesoporous thin films were synthesized using a reported procedure that allows to obtain larger pore size using a low-cost polymer as a second porogen agent (PPG = polypropylene glycol 4000—Alfa Aesar GmbH&Co) [25]. Molar ratios in the precursor sols were $\text{TiCl}_4:\text{BuOH}:\text{H}_2\text{O}:\text{F127}:\text{PPG} = 1:40:10:4 \times 10^{-3}:6.2 \times 10^{-3}$. To coat the glass substrates we used a dip-coating process at a withdrawal rate of 0.5 mm s^{-1} and a relative humidity (RH) of 20%. After deposition, the films were placed in 50% RH chambers for 24 h, the films were then subjected to a consolidation thermal treatment, which consisted of heating for 24 h at 60 °C, then 130 °C, and finally 2 h at 200 °C. Next, the SiO_2 mesoporous layer was incorporated in second stages onto the stabilized titania film [24]. $\text{Si}(\text{OEt})_4$ (TEOS) was used as the inorganic precursor and F127 was selected as the template. TEOS was prehydrolyzed by refluxing for 1 h in a water/ethanol solution; $[\text{H}_2\text{O}]/[\text{Si}] = 1$; $[\text{EtOH}]/[\text{TEOS}] = 5$. To this prehydrolyzed solution was added surfactant, alcohol, and acidic water in order to prepare the precursor solutions, with final composition $\text{TEOS}:\text{EtOH}:\text{H}_2\text{O}$ (0.1 M HCl):F127 equal to 1:40:5:0.0075 mol ratios. After deposition by dip-coating at 40–50% relative humidity (RH) and 2 mm s^{-1} withdrawal rate, as-prepared films were placed in a 50% RH chamber for 24 h [24,25,34]. The films were then subjected to a consolidation thermal treatment, which consisted of

heating at 60 °C for 24 h and at 130 °C for another 24 h and finally at 350 °C during 2 h in order to remove the templating agents.

4.1. Photodeposition of silver NPs

The films were immersed in a 1 M AgNO_3 water-ethanol solution (1:1 vol. ratio) for at least 10 min under agitation in the dark. Films were subsequently placed in a plastic container and covered with the Ag^+ solution and located 2 cm beneath the UV lamp (Philips 15 W, $\lambda_{\text{max}} = 355 \text{ nm}$) for 90 min [6,7]. After deposition the sample was retired from the bath and thoroughly rinsed with water and ethanol.

4.2. Enzyme immobilization and activity

Amyloglucosidase (γ -amylase) from *Aspergillus niger* (60 U mg^{-1} solid), Glucose oxidase (GOx) from *A. niger* (181 U mg^{-1} solid) and Laccase from *Trametes versicolor* (14 U mg^{-1} solid) were purchased from Sigma-Aldrich and used without further purification. Protein immobilization was achieved by immersing the so-prepared bilayered mesoporous films in a 1 mg/ml enzyme aqueous solution for overnight under agitation at room temperature. The films were then thoroughly rinsed with water and stored in a clean box at ambient conditions. The concentrations of enzyme in the solution before and after protein adsorption were determined by UV-vis spectroscopy at 280 nm [32] and the Lowry method [33]. The enzymatic activity of immobilized amylase was determined by the starch-iodine colorimetric method [4,29].

4.3. Instrumentation

The electrochemical characterization and the biofuel cell tests were performed with a TEQ-03 Potentiostat/Galvanostat. All electrochemical experiments were carried out in a conventional three-electrode cell except for the biofuel cell experiments. A Pt

wire and a saturated calomel electrode (SCE) were used as counter electrode and reference electrode, respectively. All runs were carried out in triplicate at a constant temperature, using a water bath. Transmission electron microscopy (TEM) images were obtained using a Phillips CM 200 electron microscope. Field emission-scanning electron microscopy (FE-SEM) images were taken with a Zeiss Leo 982 Gemini electron microscope using the secondary-electron mode and an in-lens detector to improve resolution. Film thickness, porous volume and pore size distribution values were obtained from environmental ellipsometric porosimetry (EEP, SOPRA GES5A).

Acknowledgments

We acknowledge valuable discussions with P. Catalano. This work was supported by CONICET (PIP 00186) and ANPCyT (PICT 1848). S. M. acknowledges CONICET for a doctoral scholarship. M.G.B. and G. J. A. A. S-I are members of CONICET.

Appendix A. Supplementary data

Supplementary data associated with this article can be found, in the online version, at <http://dx.doi.org/10.1016/j.mtcomm.2016.04.002>.

References

- [1] C. Sanchez, C. Boissière, D. Grosso, C. Laberty, L. Nicole, Design synthesis, and properties of inorganic and hybrid thin films having periodically organized nanoporosity, *Chem. Mater.* 20 (2008) 682–737.
- [2] P. Innocenzi, L. Malfatti, Mesoporous thin films: properties and applications, *Chem. Soc. Rev.* 42 (2013) 4198–4216.
- [3] M.G. Bellino, I. Tropper, H. Duran, A.E. Regazzoni, G.J.A.A. Soler-Illia, Polymerase-functionalized hierarchical mesoporous titania thin films: towards a nanoreactor platform for DNA amplification, *Small* 6 (2010) 1221–1225.
- [4] M.G. Bellino, A.E. Regazzoni, G.J.A.A. Soler-Illia, Amylase-functionalized mesoporous silica thin films as robust biocatalyst platforms, *ACS Appl. Mater. Interfaces* 2 (2010) 360–365.
- [5] N. Frančič, M.G. Bellino, G.J.A.A. Soler-Illia, A. Lobnik, Mesoporous titania thin films as efficient enzyme carriers for paraoxon determination/detoxification: effects of enzyme binding and pore hierarchy in biocatalyst activity and reusability, *Analyst* 139 (2014) 3127–3136.
- [6] E.D. Martínez, M.G. Bellino, G.J.A.A. Soler-Illia, Patterned production of silver-mesoporous titania nanocomposite thin films using lithography-assisted metal reduction, *ACS Appl. Mater. Interfaces* 1 (2009) 746–749.
- [7] E.D. Martínez, L. Granja, M.G. Bellino, G.J.A.A. Soler-Illia, Electrical conductivity in patterned silver-mesoporous titania nanocomposite thin films: towards robust 3D nano-electrodes, *Phys. Chem. Chem. Phys.* 12 (2010) 14445–14448.
- [8] P.C. Angelomé, L.M. Liz-Marzán, Synthesis and applications of mesoporous nanocomposites containing metal nanoparticles, *J. Sol–Gel Sci. Technol.* 70 (2014) 180–190.
- [9] R.J.A. Wanders, H.R. Waterham, Biochemistry of mammalian peroxisomes revisited, *Annu. Rev. Biochem.* 75 (2006) 295–332.
- [10] C.M. O'Connor, J.U. Adams, *Essentials of Cell Biology*, NPG Education, Cambridge, MA, 2010.
- [11] P. Walde, S. Ichikawa, Enzymes inside lipid vesicles: preparation, reactivity and applications, *Biomol. Eng.* 18 (2001) 143–177.
- [12] Z. Dai, J. Bao, X. Yang, H. Ju, A bienzyme channeling glucose sensor with a wide concentration range based on co-entrapment of enzymes in SBA-15 mesopores, *Biosens. Bioelectron.* 23 (2008) 1070–1076.
- [13] H. Baumler, R. Georgieva, Coupled enzyme reactions in multicompartiment microparticles, *Biomacromolecules* 11 (2010) 1480–1487.
- [14] Y. Liu, J. Du, M. Yan, M.Y. Lau, J. Hu, H. Han, O.O. Yang, S. Liang, W. Wei, H. Wang, J. Li, X. Zhu, L. Shi, W. Chen, C. Ji, Y. Lu, Biomimetic enzyme nanocomplexes and their use as antidotes and preventive measures for alcohol intoxication, *Nat. Nanotechnol.* 8 (2013) 187–192.
- [15] I. Willner, Y.-M. Yan, B. Willner, R. Tel-Vered, Integrated enzyme-based biofuel cells—a review, *Fuel Cells* 1 (2009) 7–24.
- [16] M.H. Osman, A.A. Shah, F.C. Walsh, Recent progress and continuing challenges in bio-fuel cells. Part I: enzymatic cells, *Biosens. Bioelectron.* 29 (2011) 3087–3102.
- [17] M.J. Cooney, V. Svoboda, C. Lau, G. Martina, S.D. Minter, Enzyme catalysed biofuel cells, *Energy Environ. Sci.* 1 (2008) 320–337.
- [18] P.N. Catalano, A. Wolosiuk, G.J.A.A. Soler-Illia, M.G. Bellino, Wired enzymes in mesoporous materials: a benchmark for fabricating biofuel cells, *Bioelectrochemistry* 106 (2015) 14–21.
- [19] F. Börnke, S. Sonnewald, Biosynthesis and metabolism of starch and sugars, in: H. Ashihara, A. Crozier, A. Komamine (Eds.), *Plant Metabolism and Biotechnology*, John Wiley & Sons, Ltd., Chichester, UK, 2011.
- [20] Q. Lang, L. Yin, J. Shi, L. Li, L. Xia, A. Liu, Co-immobilization of glucoamylase and glucose oxidase for electrochemical sequential enzyme electrode for starch biosensor and biofuel cell, *Biosens. Bioelectron.* 51 (2013) 158–163.
- [21] C.-M. Yu, L.-C. Chen, Turning glucose and starch into electricity with an enzymatic fuel cell, engineering in agriculture, *Environ. Food* 2 (2009) 1–6.
- [22] K. Yamamoto, T. Matsumoto, S. Shimada, T. Tanaka, A. Kondo, Starchy biomass-powered enzymatic biofuel cell based on amylases and glucose oxidase multi-immobilized bioanode, *New Biotechnol.* 30 (2013) 531–535.
- [23] M.G. Bellino, G.J.A.A. Soler-Illia, Nano-designed enzyme-functionalized hierarchical metal-oxide mesoporous thin films: en route to versatile biofuel cells, *Small* 10 (2014) 2834–2839.
- [24] P.C. Angelomé, M.C. Fuertes, G.J.A.A. Soler-Illia, Multifunctional, multilayer, multiscale: integrative synthesis of complex macroporous and mesoporous thin films with spatial separation of porosity and function, *Adv. Mater.* 18 (2006) 397–400.
- [25] L. Malfatti, M.G. Bellino, P. Innocenzi, G.J.A.A. Soler-Illia, One-pot route to produce hierarchically porous titania thin films by controlled self-assembly swelling, and phase separation, *Chem. Mater.* 21 (2009) 2763–2769.
- [26] M.D. Gouda, S.A. Singh, A.G.A. Rao, M.S. Thakur, N.G. Karanth, D. Harrison, Thermal inactivation of glucose oxidase, *J. Biol. Chem.* 278 (2003) 24324–24333.
- [27] M.E. Calvo, N. Hidalgo, R. Schierholz, G.J.A.A. Soler-Illia, H. Míguez, Full solution processed mesostructured optical resonators integrating colloidal semiconductor quantum dots, *Nanoscale* 7 (2015) 16583–16589.
- [28] U. Specka, F. Mayer, G. Antranikian, Purification and properties of a thermoactive glucoamylase from *Clostridium thermosaccharolyticum*, *Appl. Environ. Microbiol.* 57 (1991) 2317–2323.
- [29] B.W. Smith, J.H.A. Roe, Photometric method for the determination of α -amylase in blood and urine, with the use of the starch-iodine color, *J. Biol. Chem.* 179 (1949) 53–59.
- [30] A. Zebda, L. Renaud, M. Cretin, F. Pichot, C. Innocent, R. Ferrigno, S. Tingry, A microfluidic glucose biofuel cell to generate micropower from enzymes at ambient temperature, *Electrochem. Commun.* 11 (2009) 592–595.
- [31] C. Tan, S. Saurabh, M.P. Bruchez, R. Schwartz, P. LeDuc, Molecular crowding shapes gene expression in synthetic cellular nanosystems, *Nat. Nanotechnol.* 8 (2013) 602–608.
- [32] Y.-J. Han, G. Stucky, A. Butler, Mesoporous silicate sequestration and release of proteins, *J. Am. Chem. Soc.* 121 (1999) 9897–9898.
- [33] O.H. Lowry, N.J. Rosebrough, A.L. Farr, R.J. Randall, Protein measurement with the Folin-Phenol reagents, *J. Biol. Chem.* 193 (1951) 265–275.
- [34] G.J.A.A. Soler-Illia, P.C. Angelomé, M.C. Fuertes, D. Grosso, C. Boissiere, Critical aspects in the production of periodically ordered mesoporous titania thin films, *Nanoscale* 4 (2012) 2549–2566.